ELSEVIER

Journal of Alloys and Compounds 239 (1996) 77–82

Journal of
ALLOYS
AND COMPOUNDS

Phase diagram of the binary erbium–silicon system and physical properties of erbium silicides up to 1050°C

S.P. Luzan*, V.E. Listovnichii, Yu.I. Buyanov, P.S. Martsenyuk

I.N. Frantsevich Institute for Problems of Materials Science, Academy of Science of Ukraine, Kiev 252180, Ukraine

Received 29 May 1995

Abstract

The constitutional diagram of the Er–Si system is investigated for the first time. The phase diagram has been established by means of differential thermal, X-ray and metallographic analyses. Five intermetallic compounds were found to exist in the Er–Si system: Er_5Si_3, Er_5Si_4, $ErSi_{1-x}$, ErSi and the Si-deficient compound $ErSi_{2-b}$. The paths of formation and the phase transformation temperatures of all intermetallic compounds have been determined. The silicide $ErSi_{2-b}$ is dimorphous.

The electrical resistivity of both as-cast and heat-treated alloys was investigated at room temperature. In addition, the temperature dependencies of the electroresistivity and thermal expansion of alloys close in composition to the erbium silicides were studied at temperatures up to 1050°C.

Keywords: Phase diagram; Er–Si system; Er–Si intermetallics; Resistivity; Thermal expansion

1. Introduction

The silicides of rare earth (RE) metals are promising materials that may find applications in atomic technology, the chemical industry, metallurgy and, primarily, microelectronics [1,2]. In a previous paper [3] we reported the results of a phase diagram investigation of the Ho–Si system, including an investigation of some physical properties of Ho–Si alloys. The present article describes an analogous investigation of the Er–Si system.

A complete phase diagram for the erbium–silicon system has not been given. It has been established [4] that the Er-richest compound Er_5Si_3 melts congruently and forms a eutectic at 1200°C with the solid solution of Si in Er (15 at.% Si at the eutectic point). It has also been established [5] that there is a Si-rich eutectic. It was determined that the melting point of this eutectic is 1180°C and the composition is 81 at.% Si. The composition and crystal structure of the phase in equilibrium with the Si solid solution were not investigated.

According to the literature, four erbium silicides form in Er–Si alloys: Er_5Si_3 [6–8], Er_5Si_3 [7, 9, 10], ErSi [7,11–13] and $ErSi_2$ [7,14–21]. For erbium monosilicide, the CrB-type orthorhombic structure has been established [12] and confirmed [7,13]. It is noted [13] that annealing of a compound of the equiatomic composition does not change its crystal structure. In spite of this another FeB-type modification for ErSi was found by Hohnke and Parthé [11]. These authors ascribed the FeB-type structure to a high-temperature modification, and that of the CrB-type to a low-temperature modification.

The data on the Si-richest erbium silicide compositions are not unequivocal. Several authors [16–19] found the alloy with 66.7 at.% Si to be single phase, which corresponds to $ErSi_2$. However, it was shown [7,14,15,20,21] that single phase alloys actually contain less silicon corresponding to the formula Er_3Si_5 (62.5 at.% Si), or $ErSi_{2-x}$. It was found that the crystal lattice of $ErSi_{\sim 2}$ does not belong to the hexagonal symmetry. In Refs. [7,14,16–19] it was shown that it is of the AlB_2 structure type. Investigation made with a high-temperature X-ray camera showed that from 20°C to 1200°C the silicide does not undergo any polymorphic change [22]. When studying crystal structure of as-cast Er–Si alloys containing from 50 to 66.7 at.% Si (by powder and monocrystal diffraction methods) Ghetta et al. [20], contrary to other re-

---

* Corresponding author.

SSDI 0925-8388(95)01977-4

searchers, found an orthorhombic crystal lattice in $ErSi_{2-x}$ ($x = 0.8$; 54.5 at.% Si). These authors found the crystal structure to be a superstructure of the AlB_2-type. The small orthorhombic deformation of the initially AlB_2-type lattice occurs due to difference in the occupation of the two Si positions. An analogous superstructure was found [21] for Er_3Si_5 at 15 K by powder neutron diffraction. There are no data on melting points and polymorphic transformation points for erbium silicides. In most cases nothing is reported about their mode of formation in the literature. Therefore it was felt to be necessary to investigate phase equilibria in the Er–Si system and to construct the corresponding complete phase diagram.

Electrophysical properties of RE silicides at high temperatures were studied very superficially; only the properties of RE disilicides were studied in some detail, while the metal-rich alloys were hardly investigated.

2. Experimental procedures

To prepare the alloys we used erbium (nominal purity 99.8 wt%) and monocrystalline silicon (nominal purity 99.999 wt%). The alloys were cast in an arc furnace on a water-cooled copper hearth under purified argon. To obtain alloys of homogeneous composition the ingots were turned over and remelted three times. Chemical analyses of as-cast and annealed alloys did not discover any substantial deviation from the weighted amounts. The alloys were annealed to give a homogeneous state for 250 h at a temperature of 1100°C in tantalum crucibles under purified argon.

The phase diagram of the Er–Si system was investigated by differential thermal analysis (DTA), X-ray diffraction (X-ray powder method using filtered Cr-$K\alpha_1$ radiation) and metallography. Lattice parameters for the various compounds were obtained by using the program PRC designed in our laboratory.

Because the preparation of pure Er silicides involves difficult techniques, the evaluation of the physical properties of the silicides was carried out on alloys close in composition to those silicides, which had been tested earlier, together with alloys used to construct the phase diagram. The measurements of the resistivity (ρ) and the thermal expansion ($\Delta L/L$)) were carried out on cast and annealed alloys. To take the measurements and for the accumulation and processing of the data we used the automatic system MERA on the SOU-6 computer [23]. Measurements of the electrical resistivity at room temperature were made by the four-probe method with a "stepping probe". High temperature measurements of the physical properties of the alloys were performed in purified helium or under high vacuum (the latter, starting from 400°C) at a heating rate of 10°C min^{-1}.

3. Results and discussion

The complete phase diagram for the binary erbium–silicon system has been constructed for the first time (Fig. 1). The intermediate phases in this system are the five compounds Er_5Si_3, Er_5Si_4, $ErSi_{1-x}$, ErSi and the Si-deficient compound $ErSi_{2-b}$. Data on the crystal structure of the erbium silicides are given in Table 1. The lattice parameters of the silicide phases found by ourselves are in good agreement with those reported in literature.

The silicide Er_5Si_3 melts congruently at 1948°C. The monophase structure of cast alloy containing 36.9 at.%Si (the phase Er_5Si_3) is shown in Fig. 2(a). The eutectic reaction $L \rightarrow \langle Er \rangle + Er_5Si_3$ occurs at 1288°C according to our data, which is 88°C higher than the value reported in Ref. [4]. The composition in the eutectic point determined by us (12.5 at.%, Si) is close to that reported in Ref. [4]. The microstructure of a pre-eutectic alloy is shown in Fig. 2(b). The silicide Er_5Si_4 melts incongruently at 1875°C according to the reaction $Er_5Si_4 \rightarrow Er_5Si_3 + L$. The silicides Er_5Si_4 and

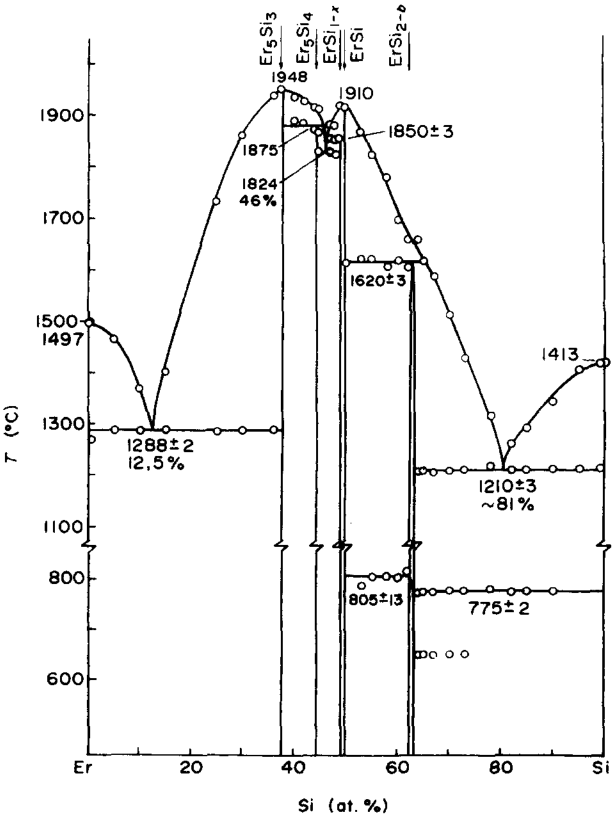

Fig. 1. Phase diagram of the erbium–silicon binary system: ○– data of thermal analysis.

Table 1
Crystal structures and lattice parameters of Er silicides

Silicide	Phase symmetry	Structural type	Lattice parameters (nm)		
			a	*b*	*c*
Er_5Si_3	*P*6_3*/mcm*	Mn_5Si_3	0.8309 ± 0.0003	—	0.6234 ± 0.0002
Er_5Si_4	*Pnma*	Sm_5Ge_4	0.728 ± 0.005	1.437 ± 0.016	0.7595 ± 0.0016
$ErSi_{1-x}$	*Cmcm*	CrB	0.4196 ± 0.0003	1.0382 ± 0.0003	0.3787 ± 0.0004
ErSi	*Pnma*	FeB	0.7777 ± 0.0007	0.3784 ± 0.0001	0.5607 ± 0.0003
$ErSi_{2-b}$	*P6/mmm*	AlB_2	0.38006 ± 0.00024	—	0.40856 ± 0.00008

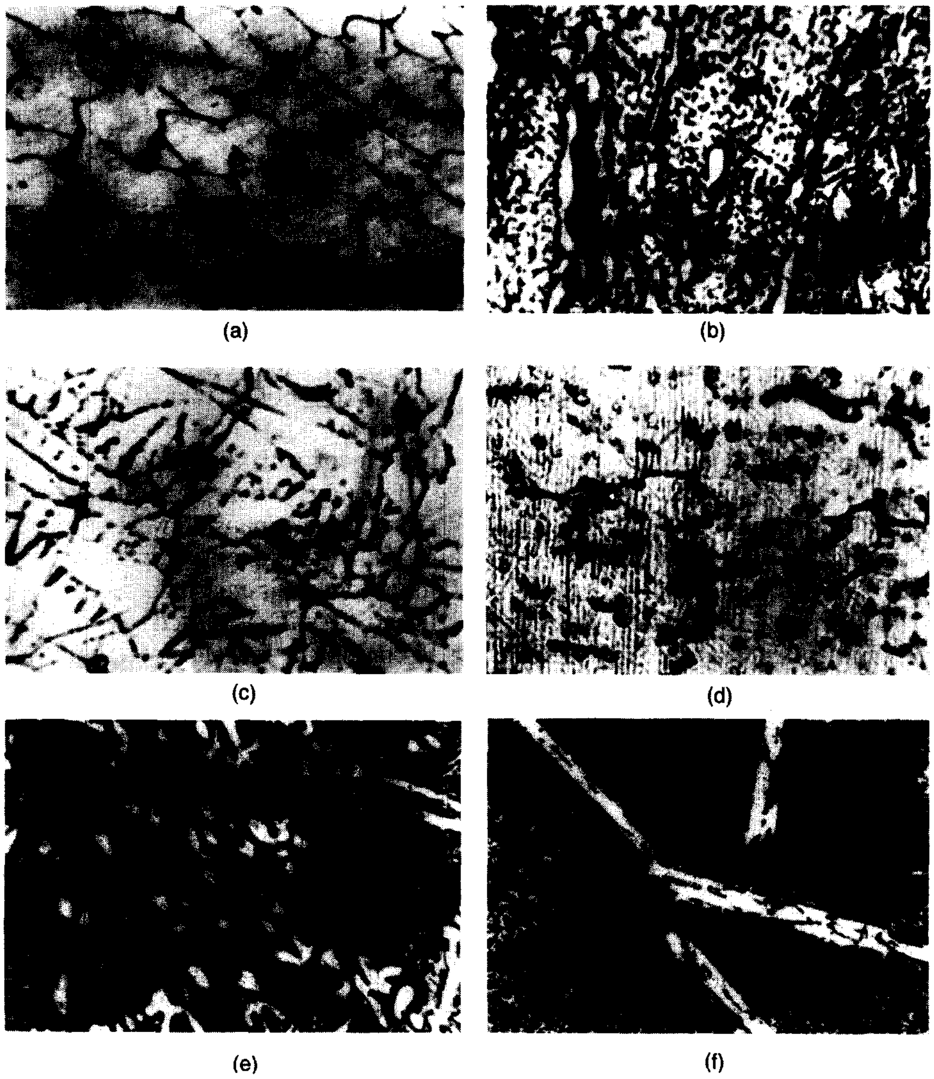

Fig. 2. Microstructure of various alloys of the Er–Si system: (a) 36.9 at.% Si, cast, Er_5Si_3 (×100); (b) 10.0 at.% Si, cast, ⟨Er⟩ + eutectic (⟨Er⟩ + Er_5Si_3) (×100); (c) 50.0 at.% Si, annealed, ErSi (×100); (d) 63.5 at.% Si, annealed, $ErSi_{2-b}$ (×100); (e) 78.2 at.% Si, annealed, $ErSi_{2-b}$ + eutectic ($ErSi_{2-b}$ + ⟨Si⟩) (×200); (f) 85.0 at.% Si, cast, ⟨Si⟩ + eutectic ($ErSi_{2-b}$ + ⟨Si⟩) (×100).

$ErSi_{1-x}$ crystallize together from the melt containing 46 at.% Si at a temperature of 1824°C.

According to our data there exist two silicides close to the equiatomic composition in the Er–Si system: the silicide $ErSi_{1-x}$ ($x \approx 0.04$) with an orthorhombic lattice of the CrB type containing 49 at.% Si and the silicide ErSi with an orthorhombic lattice of the FeB-type (see Table 1). In the alloy containing 49 at%. Si the phase of FeB-type crystallizes first. The silicide $ErSi_{1-x}$ forms peritectically by the reaction $L + ErSi \rightarrow ErSi_{1-x}$ at 1850°C. Due to rapid cooling in the arc furnace the peritectic process of the $ErSi_{1-x}$ formation is not completed and there remains some ErSi, which crystallizes initially. This may account for the fact that two different structures of the monosilicide (CrB- and FeB-type) were found in the same ingot both in our experiments and in those reported in Ref. [8]. ErSi melts congruently at 1910°C. The microstructure of the annealed alloy containing 50.0 at.% Si (see Fig. 2(c)) consists almost only of the ErSi-phase. According to our data the CrB- and FeB-type phases exist not at different temperatures but at different silicon contents.

The silicide $ErSi_{2-b}$ ($b \approx 0.33$) forms by a peritectic reaction $L + ErSi \rightarrow ErSi_{2-b}$ at a temperature of 1620°C. The phase based on this silicide has a homogeneity range of about 1 at.%. The microstructure of the annealed alloy containing 63.5 at.% Si (see Fig. 2(d)) is almost single phase. We found that the silicide $ErSi_{2-b}$ is dimorphous. The temperature of the α-$ErSi_{2-b} \rightarrow \beta$-$ErSi_{2-b}$ transformation drops from 805°C to 775°C when going from the Er-rich side to the Si-rich side. X-Ray powder diffraction on $ErSi_{2-b}$ (as-cast and annealed samples) showed that the strong reflections belong to the hexagonal lattice of AlB_2 type. However there are weak superstructure reflections apparently caused by the lowering of the symmetry during transfer from the high-temperature (β) to the low temperature (α) modification of $ErSi_{2-b}$. The type of the superstructure for this silicide has not yet been determined. The nature of weak heat effects, which are detected in the thermal curves at 645°C in the alloys corresponding to the two-phase region ($ErSi_{2-b} + \langle Si \rangle$) (see Fig. 1), has not yet been determined. The silicide $ErSi_{2-b}$ crystallizes together with Si from the melt containing 81 at.% Si at 1210°C. These values are in good agreement with the data presented in Ref. [5]. The microstructures of pre- and post-eutectic alloys are shown in Figs. 2(e) and 2(f).

The system is characterized by the eutectic reactions:

$L(12.5 \text{ at.\% Si}) \rightleftharpoons \langle Er \rangle + Er_5Si_3$ at 1288°C

$L(46 \text{ at.\% Si}) \rightleftharpoons Er_5Si_4 + ErSi_{1-x}$ at 1824°C

$L(81 \text{ at.\% Si}) \rightleftharpoons \beta\text{-}ErSi_{2-b} + \langle Si \rangle$ at 1210°C

The solid solubility of erbium in silicon and that of silicon in erbium are both negligible (< 1 at.%).

The concentration dependencies of the resistivity of as-cast and annealed alloys of the Er–Si system at room temperature are shown in Fig. 3. There are noticeable maxima in the resistivity at the compositions, corresponding to the intermediate phases in the Er–Si system. Strong differences in resistivity between annealed and as-cast alloys for the concentration ranges 39–45 at.% Si and 60–70 at.% Si are noticed. The erbium silicides in these parts of the phase diagram form by peritectic reactions, which are incomplete during the rapid crystallization of the as-cast alloys. Therefore the non-equilibrium state of these alloys leads to relatively high values for the resistivity. Upon annealing the alloys reach their equilibrium. It should be noted that the value of ρ obtained by ourselves for Er at room temperature is in good agreement with that reported in literature [22].

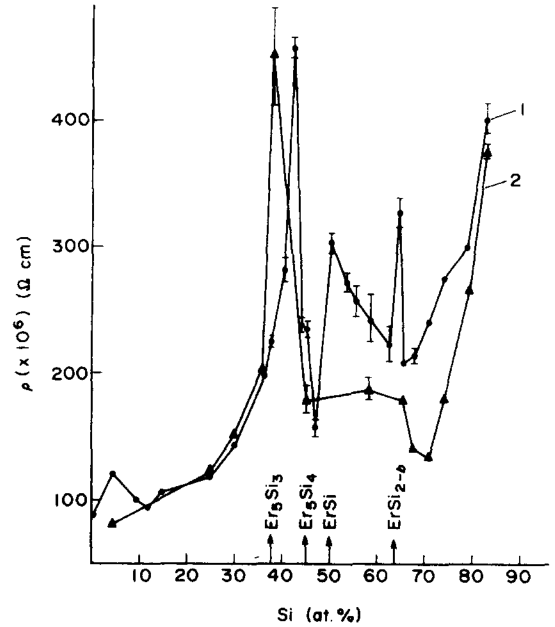

Fig. 3. Resistivity–concentration curves of Er–Si alloys: (1) as-cast alloys; (2) annealed alloys.

The temperature dependencies of the resistivity and the thermal expansion were studied on annealed alloys of the Er–Si system. For the alloys below 30 at.% Si a monotonous increase in resistivity with temperature up to 1050°C is noted (see Fig. 4), but when the Si-content in the alloys is about 30 at.% Si or larger (see Fig. 5) the character of the temperature dependencies changes and maxima appear in heating curves in the region ~550–750°C. Together with the appear-

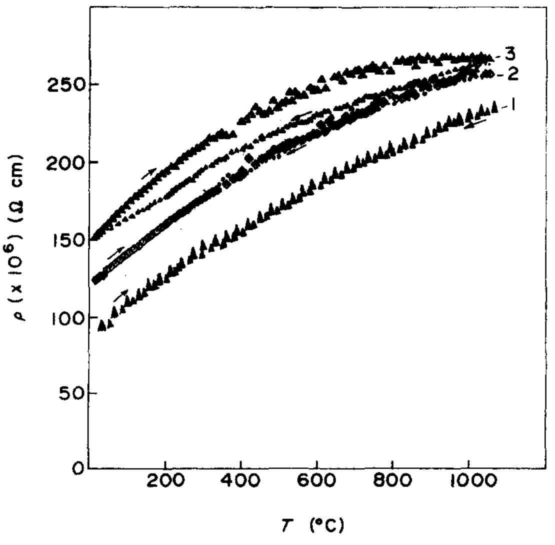

Fig. 4. Temperature dependencies (heating and cooling) of the resistivity of annealed alloys: 1–15 at.% Si; 2–25 at.% Si; 3–30 at.% Si.

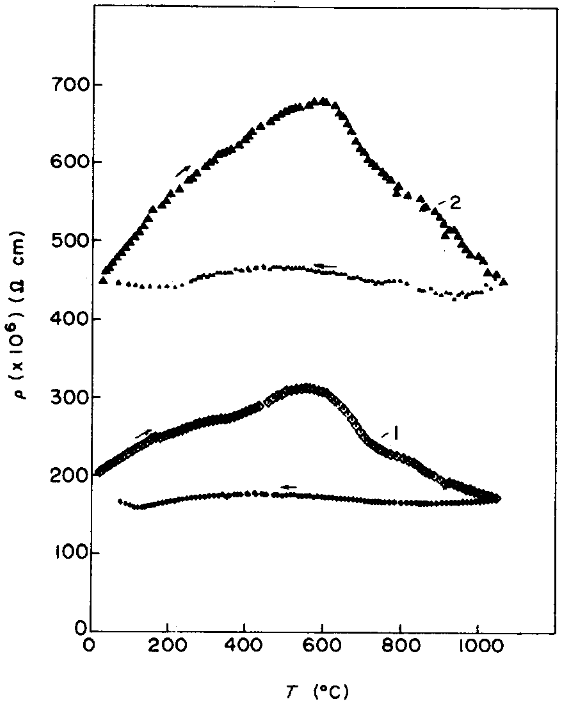

Fig. 5. Temperature dependencies (heating and cooling) of the resistivity of annealed alloys close in composition to Er_5Si_3 (1) and Er_4Si_4 (2): 1–37 at.% Si, 2–45 at.% Si.

ance of the maxima a hysteresis between the heating and the cooling curves is noted. The values of the hysteresis for the erbium silicides at first rise with increasing Si content (up to about 45 at.% Si), but then decrease for the higher silicide of Er (see Fig. 6). There are abrupt deviations in the temperature dependencies of thermal expansion at about 775°C for alloys close in composition to the Er disilicide. These correspond to the polymorphic transformation α-$ErSi_{2-b} \rightarrow \beta$-$ErSi_{2-b}$ and coincide with the abrupt changes in resistivity curves. This temperature is also in good agreement with the DTA data.

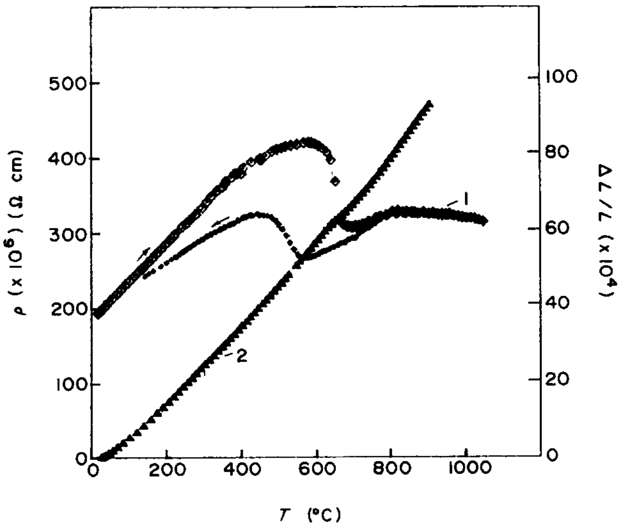

Fig. 6. Temperature dependencies (heating and cooling) of the resistivity (1) and thermal expansion (2) of annealed alloy (65 at.% Si) close in composition to $ErSi_{2-b}$.

The general picture of the temperature dependencies of resistivity for the alloys of the Er–Si system is similar to the system Ho–Si which is described elsewhere [3]. This is not surprising in view of the similarity in phase equilibria and the isomorphism of the silicides. On the basis of the investigation of the physical properties of the Ho–Si and Er–Si systems, which are partially described in the present paper, one can draw the conclusion that the intermediate phases formed by heavy RE (Ho, Er) with silicon are characterized by similar anomalies in the temperature dependencies of the resistivity. There are also characteristic smooth maxima in the $\rho(T)$ curves over the temperature interval ~500–800°C during heating, which differ from one alloy to another as to the temperatures and the values of ρ. The appearance of these maxima is not connected, as a rule, with phase changes, this having been suggested by the detailed studies of phase equilibria in the alloys. Another characteristic feature of the investigated dependencies of resistivity on temperature in the interval 20–1050°C for the alloys close in composition to the RE silicides is the quite strong hysteresis between the heating and the cooling curves. The probable reasons for the anomalous temperature dependencies of resistivity and the hysteresis phenomena on heating/cooling may be the processes of depositing–solving of the impurity admixture phases in the grain boundaries during the temperature changes or ordering–disordering of the atoms in the alloys, during the temperature changes. Therefore it is necessary to reinvestigate the temperature dependencies of resistivity on monocrystal line samples and to study the alloys by high-temperature X-ray diffraction.

References

[1] S.P. Murarka, *Silicides for VLSI Applications*, Academic Press, New York, and references cited therein.
[2] O. Thomas, E. Houssay, A. Rouault, R. Madar and J.P. Senateur, *Appl. Surf. Sci.*, *38* (1989) 156.
[3] V.N. Eremenko, V.E. Listovnichii, S.P. Luzan, Yu.I. Buyanov and P.S. Martsenyuk, *J. Alloys Comp.*, *219* (1995) 181.
[4] M. Copeland, H. Kato, *Physics and Material Problems in Reactor Control Rods*, IAEA, Vienna, 1964, p. 295.
[5] V.N. Lozovskii and L.I. Kolesnichenko, *Izv. Akad. Nauk SSSR, Neorg. Mater.*, *17* (1981) 554 (in Russian).
[6] I. Mayer and I. Shidlovsky, *Inorg. Chem.*, *8* (1969) 1240.
[7] A. Raman, *Trans. Indian Inst. Met.*, *21* (1968) 5.
[8] E.I. Gladyshevskij, *Izv. Akad. Nauk SSSR, Neorg. Mater.*, *1* (1965) 868 (in Russian).
[9] F. Holtzberg, R Gambino and T.A. McGuire, *J. Phys. Chem. Solids*, *28* (1967) 2283.
[10] G.S. Smith, A.G. Tharp and G. Johnson, *Acta Crystallogr.*, *22* (1967) 940.

[11] D. Hohnke and E. Parthé, *Acta Crystallogr.*, *20* (1966) 572.

[12] E.I. Gladyshevskij and Krypyakevich, *Zh. Strukt. Khim.*, *5* (1964) 853 (in Russian).

[13] A. Raman and H. Steinfink, *Acta Crystallogr.*, *22* (1967) 688.

[14] E.I. Gladyshevskij, *Dokl. Akad. Nauk USSR*, *4* (1963) 886 (in Russian).

[15] Ch.E. Lundin, *Rare Earth Res. New York*, (1961) 306.

[16] I.P. Mayer, T. Yanir and Shidlovsky, *Inorg. Chem.*, *6* (1967) 842.

[17] J. Pierre, E. Siaud and D. Franchen, *J. Less-Common Met.*, *139* (1988) 321.

[18] A.G. Tharp, *J. Phys. Chem.*, *66* (1962) 758.

[19] K. Sekizawa and K. Yasukochi, *J. Phys. Soc. Jpn.*, *21* (1966) 274.

[20] V. Ghetta, E. Houssay and A. Rouault, *C.r. Acad. Sci. Ser.*, *2*, *309* (1989) 995.

[21] S. Auffret, J. Pierre and B. Lambert, *Physica B.*, *162* (1990) 271.

[22] I.P. Mayer and I. Felner, *J. Less-Common Met.*, *29* (1972) 25.

[23] V.E. Listovnichii, G.N. Feniuk and V.G. Batalin, *Zavod. Lab.*, *53* (1987) 47 (in Russian).